An Enhanced Segmentation Technique for Blood Vessel in Retinal Images

Kimmy Mehta
M.Tech Student (CSE)
Punjabi University Regional Centre for It & Mgmt.
Mohali, India

Navpreet Kaur
Asst. Professor (CSE)
Punjabi University Regional Centre for It & Mgmt.
Mohali, India

ABSTRACT
One of the major symptoms of many blood related diseases like diabetes or cardiovascular disease is the change in blood vessel features. These diseases can be detected by analyzing features of retinal vessels and proper treatment can be provided to patient in early stages of disease. Cost associated in detecting these changes and inconsistency in the detection procedure led to the automation of this process. Among other tasks, retinal blood vessel segmentation is the foremost and very challenging task from which various features are analyzed to detect the disease. In this paper, an effective blood vessel segmentation method from coloured retinal fundus images is presented. Segmentation is done by extracting the green channel from RGB retinal image. Firstly the vessel structure is estimated using morphological operations and then noise is removed using Rician Denoise method. After removing the noise, segmentation of blood vessels is carried out using thresholding method. Segmented image needs to be post-processed before considering it for examining any disease. Proposed segmentation method was evaluated on two publicly available DRIVE and STARE datasets. Segmentation process achieves high level of accuracy than most of the previous techniques. Further, results have demonstrated that the proposed method is applicable for segmenting retinal vessels and taking measurements from it. Advantages of this method are its simplicity, fast segmentation process, high efficiency and scalability to deal with coloured retinal images of high resolution.

Keywords
Blood Vessel Segmentation; Diabetic Retinopathy; Medical Retinal Imaging.

1. INTRODUCTION
The leading cause of loss of sight among the peoples of working age is Diabetic Retinopathy (DR) [1]. It is due to the complications in diabetes-mellitus but not all diabetic patients are visually impaired. It has been studied that the 2% of the total diabetic patients suffer from blindness and almost one tenth suffer severe loss in sight in a time period of 10 to 15 years [2, 3]. It has been estimated that the patients suffering from DR are going to double in 2030 as compared to year 2000. 171 million patients were suffered from DR in 2000 and the toll is suspected to go as up as 366 million in 2030 [4]. Among other causes, the main cause that led to DR is growth in glucose level in blood which results in the damage of vessel endothelium. Earliest Symptoms of DR are microaneurysms i.e. small capillary dilations. Later on, various other effects start to show up like hemorrhages, macular edema and neovascularization. In final phase, retinal detachment occur which ultimately lead to blindness.

Although, DR cannot be cured but loss of sight can be prevented if it is detected in early stages [1, 5]. However, symptoms start when loss of sight start taking place and at that time it is very hard to cure. So, one can ensure that if checking of diabetic patients by eye fundus test is done on annual basis, then DR can be detected and prevented before its growth [6]. But this solution suffers from many problems like huge number of patients and less experts. Due to which most of the patients does not get proper treatment. Also, it became a big financial problem for health department because it costs $1 billion alone in the U.S. in one year [7].

From last decade, employment of computer aided diagnosis (CAD) system is playing a major role in detecting and preventing many diseases. A CAD system designed for DR can reduce the workload of specialists by filtering out the cases which are not affected by the disease. On the other hand, this system can reduce the cost of the test by a great amount [8].

For the automation of DR diagnosis, the detection of vessels is must as anomalies in vascular structure are the most important symptoms of DR. The vessel assessment requires vascular tree segmentation as a previous step for the further assessment. False positives can be reduced by getting information about blood vessel location for the diagnosis of microaneurysm and hemorrhage [9–12]. Vascular tree segmentation also proved advantageous for the other clinical purposes: in the examination of the retinopathy of prematurity [15], arteriolar narrowing [16, 17], hypertensive retinopathy to characterize vessel tortuosity [18], to examine hypertension and cardiovascular ailments [19-21], and computer-aided laser surgery [22, 23] and many other. The vascular tree segmentation also provides vital information so as to find the fundus features i.e. optic disc [24-26] and the favoea [27]. In addition to this, vascular segmentation can also be used to register multimodal images [13, 14].

Rest of the paper is presented as follows: previous work done for the segmentation of blood vessels is presented in Section 2. Materials and datasets required for the evaluation of the proposed system are discussed in Section 3. Section 4 presents the methodology applied to segment the blood vessels from retinal images. Then results are evaluated and discussed in Section 5. Finally the paper is concluded in Section 6.

2. RELATED WORK
Several methods for retinal vessel segmentation have been introduced. These can be categorized into two types: rule-based methods and supervised methods.

In case of rule-based methods, vessel tracking methods [28-33] try to get the vascular structure by following vessel middle lines. Beginning from an initial set of points established automatically or by some manual labeling, vessels are tracked by resolving from local knowledge, the most suitable candidate pixel from those near to that presently under evaluation. While other methods use mathematical morphology [15], [34-36] to aid from a priori-known vascular

shape characteristics, such as piecewise linear and connected. After this, by applying morphological operators, the vasculature is filtered from the background for the last and final segmentation. Matched filtering techniques [37-42] generally use a 2-D linear structural element with a Gaussian cross-profile section, extruded or rotated into three dimensions for identification of blood vessel cross-profile (typically a Gaussian or Gaussian-derivative profile). The kernel is oriented into many rotations (generally 8 or 12) to adjust into vessels of distinct configuration after this image is thresholded to get the vessel silhouette from the background. In case of model-based locally adaptive thresholding, a common framework based on a verification-based mutlithreshold probing technique was introduced by Jiang et al. in [43]. On the other side, snake or deformable models have also been used in [44] and [45]. A snake is a model which is active and contour, once it is placed on the image close to the contour of interest, can transform to adjust the shape of the required structure by an iterative adaption. Other rule-based methods for retinal blood vessel segmentation were introduced in [46] and [47]. Martinez et al. [46] introduced a method based upon multi-scale characteristic extraction. In the method introduced in [47], blood vessel-like structures were extracted with help of Laplacian operator and noisy structures were pruned in accordance to centerlines, detected by means of the normalized gradient vector field.

However, supervised methods are dependent on pixel classification, which based on classifying each pixel into two classes i.e. vessel and non-vessel. Classifiers are trained by supervised learning with data from manually-labeled images. Gardner et al. [48] introduced a back propagation multilayer neural network (NN) especially for vascular tree segmentation. After this histogram equalization, smoothing and edge detection, the image was split into 20 20 pixel squares (400 input neurons). The NN was then input with the values of these pixel windows for categorizing every pixel into vessel or not. Sinthanayothin et al. [49] also used a multilayer perceptron NN. Every pixel in the image was categorized by using the very first principal component, and the edge strength values from a 10 10 pixel sub-image placed on the pixel under examination, as input data. Niemeijer et al. [50] put into practice a K-nearest neighbor (k-NN) classifier. A 31-component pixel feature vector was established with the Gaussian and its derivatives up to order 2 at 5 distinct scales, augmented with the gray-level from the green channel of the real image. The assumption that the vessels are elongated structures is the base for the supervised ridge-based vessel detection process introduced by staal et al. [51]. Ridges were located from the image and then used as primitives to make line elements. Every pixel was then allotted to its closest line element, the image thus being divided into patches. For each pixel, 27 characteristics were initially computed and those providing the best class separability were finally selected. Feature vectors were categorized by using a k-NN classifier and sequential forward characteristic selection. Soares et al. [52] used a Gaussian mixture model Bayesian classifier. Multi-scale analysis was operated on the image by using the Gabor wavelet transform. The gray-level of the inverted green channel and the highest Gabor transform reaction over angles at four distinct scales were considered as pixel characteristics. Finally, Ricci and Pefetti [53] used a support vector machine (SVM) for pixel categorization as vessel or non-vessel. They used two orthogonal line detectors to construct the feature vector along with the gray-level of the target pixel.

3. MATERIALS

Popular datasets which are used for the evaluation of retinal blood vessel segmentation are DRIVE and STARE. In both datasets, images are divided into training and testing classes. Training class include the images with ground truth where the segmentation is done manually by the experts. Testing class include images which are to be tested to check the validation of the proposed system.

DRIVE dataset [54] contain 40 images taken from the colour fundus camera Canon CR5. Resolution of image is kept fixed at 768*584 pixels and format in which images are stored is TIFF. Field of view for the camera is 45° which is approximately 540 pixels and is a non mydratic 3CCD camera. The images were obtained in a screening program held in Netherlands for retinopathy diabetic. There were 453 subjects with age greater than 30 years. Testing set is divided further into set X and set Y. There are 577,649 pixels which are marked as vessels and 3,960,532 pixels which are marked as non-vessel in set X. In set Y, pixel marked as vessel is 556,532 and as non-vessel are 3,981,611 pixels.

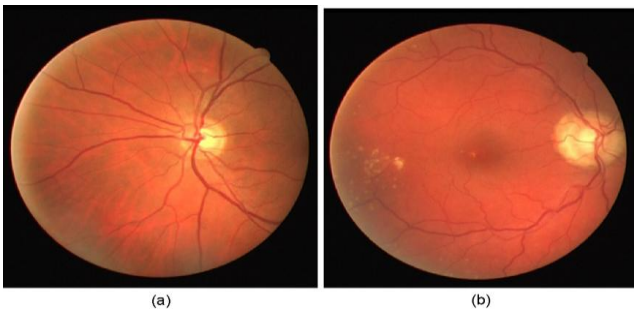

Fig. 2 DRIVE: (a) healthy image, (b) image with pathologies

STARE dataset [55] contain 20 images taken by TopCon TRV-50 camera. Resolution of images is kept at 700*605 pixels and the images are stored in a PPM format. Field of view for this dataset is 35°. Manual segmentation was done by two observers. One of them segmented 10.4% pixels as vessel while other has segmented 14.9%. The difference in the segmented pixels lies in the fact that second observer segmented more number of thinner vessels than the first one.

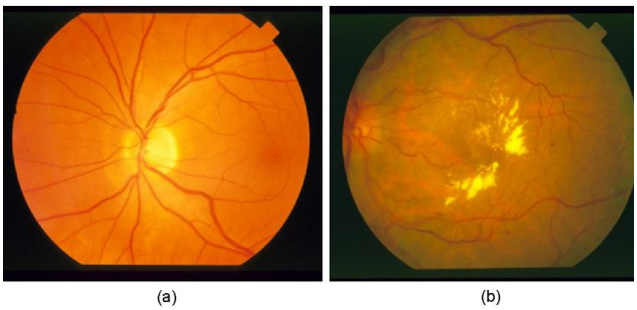

Fig. 3 STARE: (a) healthy image, (b) pathological image

4. METHODOLOGY

Proposed approach for blood vessel detection and segmentation is presented in this section. Fundus retinal images are firstly preprocessed to remove the noise and enhancing blood vessels. The segmentation of blood vessels is done by estimating vessels using morphological operations from green channel. Finally the segmentation results are compared with the ground truth to evaluate the performance of the proposed system. Design of the methodology followed is shown in Figure 4.

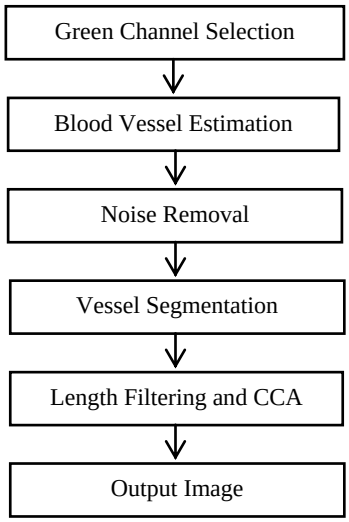

Figure 4: Proposed Segmentation Process

4.1 Green Channel Selection

The colored image of the retina is captured using fundus camera in which each color channel provides information about the anatomical and pathological structures of the retina. The vascular structure is represented using green channel as it has higher contrast between vessels and retinal background as compared to other channels and it was also considered in existing work of vessel segmentation [56-57]. Therefore, only green channel is considered for segmentation of vascular structure.

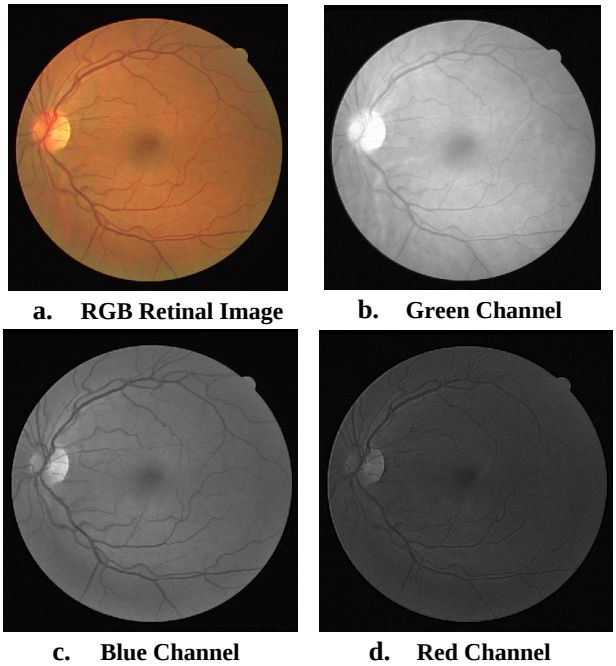

a. RGB Retinal Image **b. Green Channel**

c. Blue Channel **d. Red Channel**

Figure 5: RGB Channels of Fundus Retinal Image.

4.2 Blood Vessel Estimation

The blood vessel structure is estimated by normalizing the retinal image. It is achieved by subtracting the original image from estimated background retinal image. The background image is estimated using morphological operations. Morphological operations are collection of techniques used for extracting components that are useful for representation and description of shape regions such as boundaries, skeletons and convex hull [58]. The most basic morphological operations are dilation and erosion. On the basis of these operations morphological opening and closing operations are defined. The closing operation is given as:

$$p = (f \bullet g) = (f \oplus g) \ominus g$$

Where f is the input image, g is the structuring element, $\oplus$ denotes dilation and $\ominus$ denotes erosion. The morphological closing operation has been used in this work to estimate background of retinal area. Since closing operation suppresses dark details smaller than the structuring element. Therefore it will eliminate the vessels present in the retinal image to produce the background of retina. Here, size of the structuring element is the parametric value on which the background estimation depends. Larger the size of structuring element, more the blurred retinal image will be. Vessel structure is estimated as:

$$s = |f - p|$$

The vessel structure estimation is the absolute difference between original image and estimated background retina.

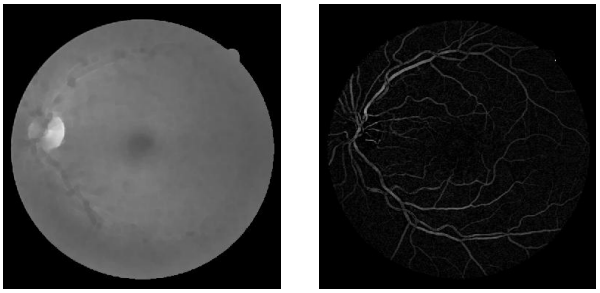

Background Estimation **Vessel estimation**

Figure 6:Blood Vessel Estimation

4.3 Noise Removal

Since noise from the original input image is not removed; it remains exists after vessel estimation. Therefore, it is required to de-noise the retinal image while preserving the vascular structure as shown in Figure 7. The process of denoising of image includes transformation of image where noise is identified easily. Then inverted transformation is applied to reconstruct the noise free image [57]. Rician denoise is a total variation based algorithm that tries to remove noises. Assuming $f = u + n$, where u is the original image; f is the observed image with Rician noise n.

Figure 7:Enhanced Image

The problem is to recover original image u from a noisy image f. The following formulation can be used:

$$\min_{u \in BV(\Omega)} \int_{\Omega} |\nabla u| dx + \lambda \int_{\Omega} \left[\frac{u^2 + f^2}{2\sigma^2} - log I_0(\frac{uf}{\sigma}) \right] dx$$

where, λ is used to balance total variation, Ω is the domain of the image, σ is distribution of the Rician noise and $I_0(.)$ is the modified Bessel function of order zero. The optimized code which solves the minimization problem is proposed by Tristan Ursell using gradient descent where gradient is given as:

$$\frac{\partial u}{\partial t} = \nabla . \frac{\nabla u}{|\nabla u|} - \frac{\lambda}{\sigma^2} u + \frac{\lambda}{\sigma^2} \frac{I_1(\frac{uf}{\sigma^2})}{I_0(\frac{uf}{\sigma^2})} f$$

The major calculations which are involved in the gradient computation are curvature term $\nabla . \frac{\nabla u}{|\nabla u|}$, where a finite difference stencil computation kernel is used in actual numeric computation [58].

4.4 Segmentation

Vascular structure of the retinal image is segmented using thresholding method proposed by Phansalkar et al. [59].

To make their method suitable for our problem, we have modified their method by setting thresholding scheme to global instead of local. It is done by setting the size of local search window to whole image. Then calculated threshold is used for segmenting the vascular structure. It is given as:

$$T = mean(f) \left[1 + pe^{-q * mean\,(f)} + k \left(\frac{std(f)}{R} - 1 \right) \right]$$

The parametric values of the method are set as: $k = 0.25$, $p = 2$, $q = 10$ *and* $R = 0.5$. The selection of these parameters is based on accuracy evaluation by selecting several combination values on individual datasets. The final set of combination which is selected is one which produces highest accuracy. These parametric values are kept fixed for all images of datasets.

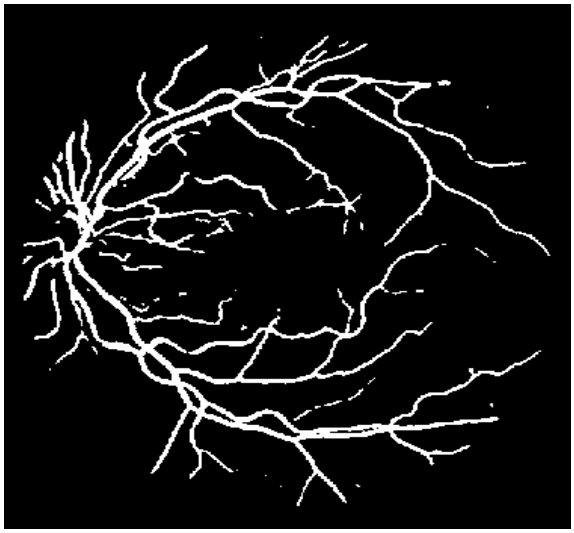

Figure 8: Segmented Image

4.5 Post Processing

Post Processing: To further increase the performance of proposed algorithm, two post processing operations are applied on segmented image. These operations are area filtering and spur pixels elimination. Area filtering is applied to remove those small isolated and unwanted regions which do not belong to vascular structure. It is done using Connected Component Analysis (CCA) technique in which image is labeled into different components based on their pixel connectivity (either with 4 or 8-way connectivity) [60]. In this work 8-way connectivity is used for labeling and then for each labeled component area is calculated to remove false regions. False regions are that whose area is less than *A*, else is vascular structure. Further, spur pixels are also removed which are presented at edges of vessel structure to obtain final output image as shown in Figure 9.

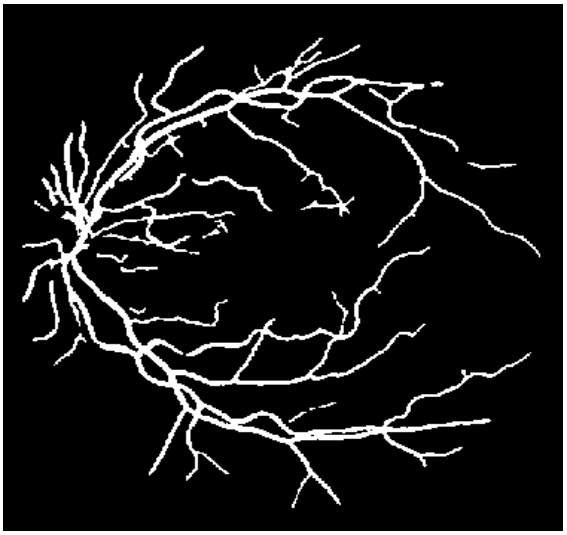

Figure 9: Final Segmented Image

5. RESULTS AND DISCUSSION

The performance of the proposed algorithm is evaluated on two publically available retinal image datasets namely, STARE and DRIVE for automatic segmentation of vascular structure. These datasets are used by many researchers to test performance of their algorithms. STARE dataset consists of total 20 colored retinal images and DRIVE dataset consists of total 40 colored retinal images divided into two sets: training and testing. Both datasets are provided with hand labeling of vessels by two different specialists. In existing work, hand labeling provided by first specialists is considered as groundtruth for performance evaluation. Also, vessel segmentation (hand labelling) provided by second specialists is evaluated against first for performance analysis.

The proposed algorithm is implemented on system having MATLAB 2016 development environment and Intel core I7 CPU running at 1.43 GHz and 8 GB RAM. It takes on an average a *sec* to process each retinal image.

We evaluated our method in terms of sensitivity (SE), specificity (SP) and accuracy (ACC) metrics which are given as:

$$SE = \frac{TP}{TP + FN}$$

$$SP = \frac{TN}{TN + FP}$$

$$ACC = \frac{TP + TN}{TP + FP + FN + TN}$$

Where *True Positive* (TP) represents correctly classified vessel pixels, *False Positive (FP)* represents non-vessel pixels

incorrectly classified as vessel, *False Negative* (FN) represents vessel pixels incorrectly classified as non-vessel and *True Negative* (TN) represents correctly classified non-vessel pixels.

The vascular structure for both datasets is extracted by setting the parameters as follows: disk structuring element for the background estimation is set to 5 and area filtering threshold is set to 50. Results obtained from proposed methodology are tabulated in Table 1 and Table 2. Further it is compared with state of the art techniques in Table 3.

Table 2: Performance Metrics for Drive Dataset

Image No.	SE	SP	ACC
1	0.751598	0.976396	0.946929
2	0.767162	0.981553	0.949433
3	0.684182	0.977028	**0.934363**
4	0.651946	0.989855	0.944801
5	0.63865	0.990249	0.942537
6	0.622582	0.987518	0.936017
7	0.679273	0.976875	0.937472
8	0.640952	0.984056	0.940932
9	**0.567988**	**0.992116**	0.9423
10	0.693503	0.982526	0.948006
11	0.666712	0.98083	0.940109
12	0.66669	0.983437	0.943789
13	0.630442	0.986812	0.93629
14	0.724306	0.980951	0.950689
15	0.754277	**0.964958**	0.943081
16	0.64402	0.984472	0.939928
17	0.668665	0.979009	0.940744
18	0.718062	0.974492	0.945038
19	**0.813461**	0.978322	**0.958481**
20	0.725684	0.976129	0.94942
Average	**0.685508**	**0.981379**	**0.943518**

It can be seen from the table 1 that proposed methodology performs segmentation with an average accuracy of 94.35% for DRIVE dataset. Further it is observed that average specificity is 98.13% and sensitivity is 68.55%.

Table 2: Performance Metrics for Stare Dataset

Image No.	SE	SP	ACC
1	0.648517	0.951438	0.918498
2	0.593353	**0.940638**	**0.90867**
3	0.751578	0.953227	0.936806
4	**0.444455**	0.991712	0.935164
5	0.720731	0.96931	0.938772
6	0.834181	0.969297	0.95749
7	**0.857677**	0.965181	0.953381
8	0.822951	0.966613	0.951936
9	0.851241	0.966791	0.954376
10	0.817413	0.9625	0.946529
11	0.817296	0.967834	0.953143
12	0.868554	0.97042	0.95967
13	0.798127	0.965653	0.94518
14	0.78545	0.968743	0.945936
15	0.699207	0.97392	0.941601
16	0.601173	0.983508	0.933169
17	0.743226	0.985312	0.955605
18	0.583248	**0.994213**	**0.965741**
19	0.650348	0.985354	0.965612
20	0.536074	0.971001	0.931404
Average	**0.72124**	**0.970133**	**0.944934**

When evaluated on STARE dataset, an average of 94.49% accuracy has been obtained. Further it is analyzed that average values for specificity is 72.12% and sensitivity is 97.01%.

Table 3: Comparison with State of the Art Techniques

Method Name	Drive	STARE
2nd Human observer	0.9471	0.9348
Jaing and Mojon [19]	0.9212	0.9009
Martinez-Perez, et al. [23]	0.9344	0.9410
Cinsdikici and Aydin [24]	0.9293	-
Fraz, et al. [25]	0.9430	0.9442
You, et al. [26]	0.9434	0.9497
Ana Salazar-Gonzalez et al. [105]	0.9412	0.9441
Staal, et al. [20]	0.9441	0.9516
Proposed Work	**0.9435**	**0.9449**

Table 3 compares the proposed method with the state of the art techniques developed for blood vessel segmentation. It can be deduced that the proposed method outperforms other and can be implemented in real world applications.

6. CONCLUSION

An enhanced technique for blood vessel segmentation from retinal images taken by fundus camera for the purpose of detecting diseases is presented in this paper. Basic morphological and thresholding methods are used for extracting the vascular structure and segmenting blood vessels respectively from green channel of the RGB retinal image. For removing noise from images, Rician Denoise technique is used. Proposed technique is implemented on two publicly available datasets, DRIVE and STARE. On evaluating the results on the basis of Sensitivity, Specificity and Accuracy, it has been found that the implemented system outperforms most of state of the art techniques and shows comparable results w.r.t. others. Obtained Sensitivity values are 68.55% and 72.12%, specificity values are 98.13% and 97.01%, and accuracy values are 94.35% and 94.49% respectively for DRIVE and STARE datasets. Simplicity, robustness and effectiveness of the proposed segmentation system and its fast implementation make it a suitable choice as a tool for being integrated into pre-screening systems for early detection of DR.

7. REFERENCES

[1] H. R. Taylor and J. E. Keeffe, "World blindness: A 21st century perspective," *Br. J. Ophthalmol.*, vol. 85, pp. 261–266, 2001.

[2] R. Klein, S. M. Meuer, S. E. Moss, and B. E. Klein, "Retinal microaneurysm counts and 10-year progression of diabetic retinopathy," *Arch. Ophthalmol.*, vol. 113, pp. 1386–1391, 1995.

[3] P. Massin, A. Erginay, and A. Gaudric, *Rétinopathie Diabétique*. New York: Elsevier, 2000.

[4] S. Wild, G. Roglic, A. Green, R. Sicree, and H. King, "Global prevalence of diabetes: Estimates for the year 2000 and projections for 2030," *Diabetes Care*, vol. 27, pp. 1047–1053, 2004.

[5] S. J. Lee, C. A. McCarty, H. R. Taylor, and J. E. Keeffe, "Costs of mobile screening for diabetic retinopathy: A practical framework for rural populations," *Aust. J. Rural Health*, vol. 8, pp. 186–192, 2001.

[6] D. S. Fong, L. Aiello, T. W. Gardner, G. L. King, G. Blankenship, J. D. Cavallerano, F. L. Ferris, and R. Klein, "Diabetic retinopathy," *Diabetes Care*, vol. 26, pp. 226–229, 2003.

[7] "Economic costs of diabetes in the U.S. in 2007," in *Diabetes Care*. : American Diabetes Association, 2008, vol. 31, pp. 596–615.

[8] American Academy of Ophthalmology Retina Panel, Preferred Practice Pattern Guidelines. Diabetic Retinopathy. San Francisco, CA, Am. Acad. Ophthalmo., 2008 [Online]. Available: http://www.aao.org/ppp

[9] T. Spencer, J. A. Olson, K. C. McHardy, P. F. Sharp, and J.V. Forrester, "An image-processing strategy for the segmentation and quantification of microaneurysms in fluorescein angiograms of the ocular fundus," *Comput. Biomed. Res.*, vol. 29, no. 4, pp. 284–302, 1996.

[10] A. J. Frame, P. E. Undrill, M. J. Cree, J. A. Olson, K. C. McHardy, P. F. Sharp, and J. V. Forrester, "A comparison of computer based classification methods applied to the detection of microaneurysms in ophthalmic fluorescein angiograms," *Comput. Biol. Med.*, vol. 28, no. 3, pp. 225–238, 1998.

[11] M. Larsen, J. Godt, N. Larsen, H. Lund-Andersen, A. K. Sjolie, E. Agardh, H. Kalm, M. Grunkin, and D. R. Owens, "Automated detection of fundus photographic red lesions in diabetic retinopathy," *Investigat. Opht. Vis. Sci.*, vol. 44, no. 2, pp. 761–766, 2003.

[12] M. Niemeijer, B. van Ginneken, J. J. Staal, M. S. A. Suttorp-Schulten, and M. D. Abramoff, "Automatic detection of red lesions in digital color fundus photographs," *IEEE Trans. Med. Imag.*, vol. 24, no. 5, pp. 584–592, May 2005.

[13] F. Zana and J. C. Klein, "A multimodal registration algorithm of eye fundus images using vessels detection and Hough transform," *IEEE Trans. Med. Imag.*, vol. 18, no. 5, pp. 419–428, May 1999.

[14] G. K. Matsopoulos, P. A. Asvestas, N. A. Mouravliansky, and K. K. Delibasis, "Multimodal registration of retinal images using self organizing maps," *IEEE Trans. Med. Imag.*, vol. 23, no. 12, pp. 1557–1563, Dec. 2004.

[15] C. Heneghan, J. Flynn, M. O'Keefe, and M. Cahill, "Characterization of changes in blood vessel width and tortuosity in retinopathy of prematurity using image analysis," *Med. Image Anal.*, vol. 6, pp. 407–429, 2002.

[16] E. Grisan and A. Ruggeri, "A divide and impera strategy for the automatic classification of retinal vessels into arteries and veins," in *Proc. 25th Int. Conf. IEEE Eng. Med. Biol. Soc.*, 2003, pp. 890–893.

[17] Y. Hatanaka, H. Fujita, M. Aoyama, H. Uchida, and T. Yamamoto, "Automated analysis of the distribuitions and geometries of blood vessels on retinal fundus images," *Proc. SPIE Med. Imag. 2004: Image Process.*, vol. 5370, pp. 1621–1628, 2004.

[18] M. Foracchia, E. Grisan, and A. Ruggeri, "Extraction and quantitative description of vessel features in hypertensive retinopathy fundus images," in *Book Abstracts 2nd Int. Workshop Comput. Asst. Fundus Image Anal.*, 2001, p. 6.

[19] X. Goa, A. Bharath, A. Stanton, A. Hughes, N. Chapman, and S. Thom, "A method of vessel tracking for vessel diameter measurement on retinal images," *Proc. ICIP*, pp. 881–884, 2001.

[20] M. E. Martinez-Perez, A. D. Hughes, A. V. Stanton, S. A. Thom, N. Chapman, A. A. Bharath, and K. H. Parker, "Retinal vascular tree morphology: A semiautomatic quantification," *IEEE Trans. Biomed. Eng.*, vol. 49, no. 8, pp. 912–917, Aug. 2002.

[21] J. Lowell, A. Hunter, D. Steel, A. Basu, R. Ryder, and R. L. Kennedy, "Measurement of retinal vessel widths from fundus images based on 2-D modeling," *IEEE Trans. Med. Imag.*, vol. 23, no. 10, pp. 1196–1204, Oct. 2004.

[22] D. E. Becker, A. Can, J. N. Turner, H. L. Tanenbaum, and B. Roysam, "Image processing algorithms for retinal montage, synthesis, mapping and real-time location determination," *IEEE Trans. Biomed. Eng.*, vol. 45, no. 1, pp. 115–118, Jan. 1998.

[23] H. Shen, B. Roysam, C. V. Stewart, J. N. Turner, and H. L. Tanenbaum, "Optimal scheduling of tracing computations for real-time vascular landmark extraction from retinal fundus images," *IEEE Trans. Inf. Technol. Biomed.*, vol. 5, pp. 77–91, Mar. 2001.

[24] A. Hoover and M. Goldbaum, "Locating the optic nerve in a retinal image using the fuzzy convergence of the blood vessels," *IEEE Trans. Med. Imag.*, vol. 22, no. 8, pp. 951–958, Aug. 2003.

[25] M. Foracchia, E. Grisan, and A. Ruggeri, "Detection of optic disc in retinal images by means of a geometrical model of vessel structure," *IEEE Trans. Med. Imag.*, vol. 23, no. 10, pp. 1189–1195, Oct. 2004.

[26] A. A. H. A. R. Youssif, A. Z. Ghalwash, and A. R. Ghoneim, "Optic disc detection from normalized digital fundus images by means of a vessels' direction matched filter," *IEEE Trans. Med. Imag.*, vol. 27, no.1, pp. 11–18, Jan. 2008.

[27] H. Li and O. Chutatape, "Automated feature extraction in color retinal images by a model based approach," *IEEE Trans. Biomed. Eng.*, vol. 51, no. 2, pp. 246–254, Feb. 2004.

[28] O. Chutatape, L. Zheng, and S. Krishman, "Retinal blood vessel detection and tracking by matched Gaussian and Kalman filters," in *Proc. IEEE Int. Conf. Eng. Biol. Soc.*, 1998, vol. 20, pp. 3144–3149.

[29] Y. A. Tolias and S. M. Panas, "A fuzzy vessel tracking algorithm for retinal images based on fuzzy clustering," *IEEE Trans. Med. Imag.*, vol. 17, no. 2, pp. 263–273, Apr. 1998.

[30] A. Can, H. Shen, J. N. Turner, H. L. Tanenbaum, and B. Roysam, "Rapid automated tracing and feature extraction from retinal fundus images using direct exploratory algorithms," *IEEE Trans. Inform. Technol. Biomed.*, vol. 3, no. 2, pp. 125–138, Jun. 1999.

[31] L. Gagnon, M. Lalonde, M. Beaulieu, and M.-C. Boucher, "Procedure to detect anatomical structures in optical fundus images," *Proc. SPIE Med. Imag.: Image Process.*, vol. 4322, pp. 1218–1225, 2001.

[32] I. Liu and Y. Sun, "Recursive tracking of vascular networks in angiograms based on the detection-deletion scheme," *IEEE Trans. Med. Imag.*, vol. 12, no. 2, pp. 334–341, Jun. 1993.

[33] L. Zhou, M. S. Rzeszotarski, L. J. Singerman, and J. M.

Chokreff, "The detection and quantification of retinopathy using digital angiograms," *IEEE Trans. Med. Imag.*, vol. 13, no. 4, pp. 619–626, Dec. 1994.

[34] T. Walter and J. C. Klein, "Segmentation of color fundus images of the human retina: Detection of the optic disc and the vascular tree using morphological techniques," in *Medical Data Analysis, ser. Lecture Notes in Computer Science*, J. Crespo, V. Maojo, and F. Martin, Eds. Berlin, Germany: Springer-Verlag, 2001, pp. 282–287.

[35] F. Zana and J. C. Klein, "Segmentation of vessel-like patterns using mathematical morphology and curvature evaluation," *IEEE Trans. Image Process.*, vol. 10, no. 7, pp. 1010–1019, Jul. 2001.

[36] A. M. Mendonça and A. Campilho, "Segmentation of retinal blood vessels by combining the detection of centerlines and morphological reconstruction," *IEEE Trans. Med. Imag.*, vol. 25, no. 9, pp. 1200–1213, Sep. 2006.

[37] S. Chaudhuri, S. Chatterjee, N. Katz, M. Nelson, and M. Goldbaum, "Detection of blood vessels in retinal images using two-dimensional matched filters," *IEEE Trans. Med. Imag.*, vol. 8, no. 3, pp. 263–269, Sep. 1989.

[38] A. Hoover, V. Kouznetsova, and M. Goldbaum, "Locating blood vessels in retinal images by piecewise threshold probing of a matched filter response," *IEEE Trans. Med. Imag.*, vol. 19, no. 3, pp. 203–210, Mar 2000.

[39] L. Gang, O. Chutatape, and S. M. Krishnan, "Detection and measurement of retinal vessels in fundus images using amplitude modified second-order Gaussian filter," *IEEE Trans. Biomed. Eng.*, vol. 49, pp. 168–172, Feb. 2002.

[40] M. Al-Rawi and H. Karajeh, "Genetic algorithm matched filter optimization for automated detection of blood vessels from digital retinal images," *Comput. Methods Programs Biomed.*, vol. 87, pp. 248–253, 2007.

[41] M. Al-Rawi, M. Qutaishat, and M. Arrar, "An improved matched filter for blood vessel detection of digital retinal images," *Comput. Biol. Med.*, vol. 37, pp. 262–267, 2007.

[42] M. G. Cinsdikici and D. Aydin, "Detection of blood vessels in ophthalmoscope images using MF/ant (matched filter/ant colony) algorithm," *Comput. Methods Programs Biomed.*, vol. 96, pp. 85–95, 2009.

158 IEEE TRANSACTIONS ON MEDICAL IMAGING, VOL. 30, NO. 1, JANUARY 2011

[43] X. Jiang and D. Mojon, "Adaptive local thresholding by verification based multithreshold probing with application to vessel detection in retinal images," *IEEE Trans. Pattern Anal. Mach. Intell.*, vol. 25, no. 1, pp. 131–137, Jan. 2003.

[44] T. McInerney and D. Terzopoulos, "T-snakes: Topology adaptive snakes," *Med. Imag. Anal.*, vol. 4, pp. 73–91, 2000.

[45] L. Espona, M. J. Carreira, M. Ortega, and M. G. Penedo, "A snake for retinal vessel segmentation," *Pattern Recognition and Image Analysis*, vol. 4478, Lecture Notes Comput. Sci., pp. 178–185, 2007.

[46] M. E. Martinez-Perez, A. D. Hughes, S. A. Thom, A. A. Bharath, and K. H. Parker, "Segmentation of blood vessels from red-free and fluorescein retinal images," *Med. Imag. Anal.*, vol. 11, pp. 47–61, 2007.

[47] B. S. Y. Lam and H. Yan, "A novel vessel segmentation algorithm for pathological retina images based on the divergence of vector fields," *IEEE Trans. Med. Imag.*, vol. 27, no. 2, pp. 237–246, Feb. 2008.

[48] G. G. Gardner, D. Keating, T. H.Williamson, and A. T. Elliott, "Automatic detection of diabetic retinopathy using an artificial neural network: A screening tool," *Br. J. Ophthalmol.*, vol. 80, pp. 940-944, 1996.

[49] C. Sinthanayothin, J. F. Boyce, H. L. Cook, and T. H. Williamson, "Automated localisation of the optic disc, fovea and retinal blood vessels from digital colour fundus images," *Br. J. Ophtalmol.*, vol. 83, pp. 902–910, 1999.

[50] M. Niemeijer, J. Staal, B. v. Ginneken, M. Loog, and M. D. Abramoff, J. Fitzpatrick and M. Sonka, Eds., "Comparative study of retinal vessel segmentation methods on a new publicly available database," in *SPIE Med. Imag.*, 2004, vol. 5370, pp. 648–656.

[51] J. Staal, M. D. Abràmoff, M. Niemeijer, M. A. Viergever, and B. V. Ginneken, "Ridge based vessel segmentation in color images of the retina," *IEEE Trans. Med. Imag.*, vol. 23, no. 4, pp. 501–509, Apr. 2004.

[52] J. V. B. Soares, J. J. G. Leandro, R. M. Cesar, Jr., H. F. Jelinek, and M. J. Cree, "Retinal vessel segmentation using the 2D Gabor wavelet and supervised classification," *IEEE Trans. Med. Imag.*, vol. 25, no. 9, pp. 1214–1222, Sep. 2006.

[53] E. Ricci and R. Perfetti, "Retinal blood vessel segmentation using line operators and support vector classification," *IEEE Trans. Med. Imag.*, vol. 26, no. 10, pp. 1357–1365, Oct. 2007.

[54] Research Section, Digital Retinal Image for Vessel Extraction (DRIVE) Database. Utrecht, The Netherlands, Univ. Med. Center Utrecht, Image Sci. Inst. [Online]. Available: http://www.isi.uu.nl/Research/Databases/DRIVE

[55] STARE ProjectWebsite. Clemson, SC, Clemson Univ. [Online]. Available: http://www.ces.clemson.edu/

[56] Joao V. B. Soares, Jorge J. G. Leandro, Roberto M. Cesar Jr., Herbert F. Jelinek, and Michael J. Cree, "Retinal Vessel Segmentation Using the 2- D Gabor Wavelet and Supervised Classification", IEEE Trans. Med. Imag., 2010.

[57] Dalwinder Singh, Dharamveer, Birmohan Singh, "New Morphology based Approach for Blood Vessel Segmentation in Retinal Images,"

[58] Rosenfeld, A., and Pfaltz, J. L. (1996) 'Sequential operations in digital picture processing', *Journal of the* ACM, Vol. 13 No. 4, pp. 471–494.

[59] Phansalkar, Neerad, Sumit More, Ashish Sabale, and Madhuri Joshi. "Adaptive local thresholding for detection of nuclei in diversity stained cytology images." In Communications and Signal Processing (ICCSP), 2011 International Conference on, pp. 218-220. IEEE, 2011.

[60] P. Getreuer, M. Tong, and L. A. Vese. A variational model for the restoration of mr images corrupted by blur and rician noise. In *Proc. ISVC*, pages 686–698, 2011.